Engineering Science and Technology, an International Journal 21 (2018) 672–678

HOSTED BY

ELSEVIER

Contents lists available at ScienceDirect

Engineering Science and Technology, an International Journal

journal homepage: www.elsevier.com/locate/jestch

Full Length Article

Numerical analysis of lift-based in-pipe turbine for predicting hydropower harnessing potential in selected water distribution networks for waterlines optimization

Temidayo Lekan Oladosu [a,b,*], Olufemi Adebola Koya [a]

[a] Department of Mechanical Engineering, Obafemi Awolowo University, Ile-Ife, P.M.B. 013, Nigeria
[b] Prototype Engineering Development Institute (NASENI), Ilesa, Osun State, Nigeria

ARTICLE INFO

Article history:
Received 26 November 2016
Revised 24 April 2018
Accepted 27 May 2018
Available online 5 June 2018

Keywords:
In-pipe
Turbine
Simulation
Optimization
Hydropower
Renewable
Water distribution
Modelling

ABSTRACT

The research models and simulates in-pipe turbine hydropower harnessing possibilities in water distribution networks of the sites under investigation considering in-pipe lift-based spherical turbine. The hydrofoil profile of the turbine is generated using National Advisory Committee for Aeronautics (NACA) aerofoil generator. Consequently, a Computer-Aided Design (CAD) model of the in-line lift-based spherical turbine is then developed and simulated, based on the peak and lean period of the volumetric discharge rates using commercial computational fluid dynamics software (Autodesk Simulation CFD®). The time series of power outputs are computed from the time series of discharge variations. A lift-based spherical turbine with NACA 0020 foil cross-section appears appropriate for extraction of energy in the water distribution pipelines. Furthermore, the minimum and maximum percentage head loss due to insertion of the turbine is about 1.94% at lean flow rates and 9.70% at the peaks for 250 mm pipelines. The available power was found out to depend on the density of the turbine blades material, flow rate, and the pipe diameter. The estimated lean and the peak electric power are about 415 and 1663 W, respectively, using aluminium foil blades while stainless steel foil produces about 242 and 1080 W in the 250 mm pipe.

1. Introduction

The need for saving water and energy had grown as one of the world main concerns over the years and are expected to become more important in the near future [1]. Small hydropower can be retrofitted into a water supply system where the design head of the turbine to be used depends on the excessive hydraulic head of the distribution lines. An innovative energy policy would necessitate the exploitation of the hydraulic power dissipated along the water distribution network. Several technical solutions have been proposed to replace pressure reducing valves with energy production devices [2] in order to allow effective power conversion and a reliable network pressure regulation of water distribution networks [3]. Carravetta reported using pump as turbine PAT's in the literature [4]. Chen researched on a novel vertical-axis water turbine for hydropower harnessing inside water pipelines, posited that the power generated was used for power supply for the data collection systems in underground and congested locations or to maintenance work at remote locations using CFD (Computational Fluid Dynamic) simulation and lab tests [5]. The energy efficiency of water supply systems can be increased through the recovery of hydraulic energy implicit to the volumes of water transported in various stages of the supply process, which can be converted into electricity through hydroelectric recovery systems. Such a process allows the use of a clean energy source that is usually neglected in water supplies, reducing its dependence on energy from the local network and the system's operation costs [6]. According to lucid technology in the patient document with patient no: US 7,959,411 where lift based turbine was proved to be efficient with little flow reduction rate, for the pipes diameter within the range of 610–1575 mm (24–62 in.). Consequently, a research that further adapts lift based turbine to smaller pipe diameter was recommended [7].

From a recent work on five blades tubular propeller turbine for pipe inline installation, it was obtained that the best efficient point (BEP) corresponds to an efficiency of around 64%, held at a rotation speed of 750 rpm, a flow of 16 m^3/h and 0.34 bar (3.5 m) of a head. The maximum mechanical power measured was around 330 W, for

* Corresponding author.
E-mail address: temidayooladosu@gmail.com (T.L. Oladosu).
Peer review under responsibility of Karabuk University.

https://doi.org/10.1016/j.jestch.2018.05.016
2215-0986/© 2018 Karabuk University. Publishing services by Elsevier B.V.

a maximum flow of 48 m^3/h, 0.48 bar of head and 1500 rpm of rotation speed [8].

The hydropower generation potential of the public universities in southwestern Nigeria, to determine those institutions equipped with the appropriate operational water distribution networks was carried out by considering hydropower potential at service reservoirs due to the possibility of appreciable power potential. Consequently, the water distribution networks of the University of Ibadan, Ibadan (UI), Obafemi Awolowo University Ile-Ife (OAU), and the Federal University of Technology Akure (FUTA) were surveyed for data collections and the volumetric discharge rates were taken in an hour interval for 24 hours [9].

The objective of this study is to model and estimate hydropower possibilities of an in-pipe turbine for water lines optimization based on time series of water distribution discharge rates and the available effective head in the water lines of the selected public universities in southwestern Nigeria. Therefore, this work will make available important data and model for related investigations. The technical feasibility of small hydropower integration will be limited to CAD modeling of existing in-pipe turbine. The turbine considered in this research is lift-based spherical turbine based on its established suitable performance in water distribution systems that do not defeat the original purpose of configuration of effective water distribution to the users at the expense of power harnessing along the water lines.

1.1. Lift based spherical turbine

In-pipe turbines were analyzed by lucid technology pipelines (Lucid, 2014) but large conduit diameters of 610–1575 mm (24–62 in.) were tested. The lift based spherical turbine is a form of turbine configuration that rotates transversely under the power of fluid flowing in the pipe, which is coupled with the appropriate generator to produce electricity. The blade of the spherical turbine curve is in an approximately 180 degree arc in a plane that is an inclined angle relatively to the rotational axis of a central shaft, therefore, the blades of the spherical turbine are airfoil in cross section to optimized the hydrodynamics flow, minimize cavitation and to maximize the conversion from axial to rotating energy [7]. The pictorial representation of this turbine is expressed by Fig. 1.

2. Material and methods

The spherical lift based in pipe turbine was model with Computer Aided Design (CAD) tool Autodesk Inventor 2015 [9] while

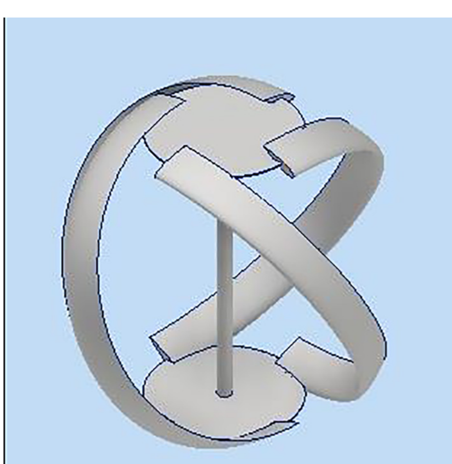

Fig. 1. Lift based spherical turbine [7].

the minimum and maximum time series of water distribution volumetric discharges taken on the investigated sites using kent volumetric water meters (Elster Kent H4000 model, England) [10] inserted along the energy lines were used as the input parameters for the numerical analysis. The pressure heads were estimated with Global Positioning System GPS (e-Trex GPS, 79; 98 Garmin model, USA) device with Wide Area Augmentation System (WAAS) receiver. The internal diameters of the pipes in the networks were measured to the nearest millimeters, using venier caliper (Mitutoyo 505 series dial caliper model, Japan). Water distribution networks of the University of Ibadan, Ibadan (UI), Obafemi Awolowo the University, Ile-Ife (OAU), and the Federal University of Technology, Akure (FUTA) were considered for data collection being institutions equipped with the appropriate operational water distribution networks in southwestern Nigeria. The numerical power output was derived from each site with the use of computational fluid dynamics software (Autodesk® Simulation CFD) [11].

2.1. Basic parameters of the lift based spherical turbine model

The parameters of the modeled lift-based in-pipe turbine are gotten from using the conduit diameter as the presiding parameter of conversion between the existing model and the adaptive model. Parameters are 0.2336 m turbine diameter, 0.1988 m turbine height, and 0.0287 m chord length, 0.1 m hub diameter with turbine shaft diameter of 0.01 m, Blockage ratio 0.11, Number of blades 4, Equatorial solidity 0.18, Average solidity 0.22, blade hydrofoil cross sectional profile takes after the standard of National Advisory Committee for Aeronautics (NACA) four digit symmetric series NACA 0020 using equation (4) to generate the 200 data with the aid of NACA 4-digit series airfoil generator tool, which in turn was exported into the Autodesk inventor during CAD modeling, Blade overlap is 2.

2.2. Simulation of the modelled turbine

The modelled turbine was simulated by importing the turbine CAD model into the simulation software for numerical computation. The CFD numerical computation was done with the use of Autodesk Simulation CFD [12]. Having imported the extraneous features free CAD geometry into Autodesk Simulation CFD as design study, the small edges and sliver surfaces on the impeller were removed with the aid of geometry preparation tool. The suction (inlet) and discharge (outlet) was extended at four hydraulic diameters from the impeller to prevent the boundary conditions from directly influencing the results. Material assignment to each part of the model was carefully carried out. The fluid domain was also created within the pipe which subsequently assigned material to as water. The rotating region that becloud the impeller was also assigned a rotating region to as material which can be preset to a known rotating speed while ramping up the rotating speed to avoid impulsive start up and later to free spinning (turbine mass moment of inertial is required in flow driven analysis) as the case may be. The initial and boundary conditions were also carefully setup at the inlet and outlet to represent the real scenario, while the inlet was set up as observed volumetric discharge in cubic meter per hour for each analysis, The outlet was set as zero static gauge pressure, while monitoring plane was setup to determine magnitude of the parameters at the downstream. Automatic-sizing tetrahedral mesh was used for the analysis. The mesh at the rotating region, inlet surface, and outlet surface were assigned uniform mesh which in turn spread to entire mesh matrixes. The model has about 3.2 million tetrahedral elements. Fluid-cap (entry length) was about two-third of the fluid domain diameter that enabled full development of fluid. Incompressible fluid was assumed, SST – k omega turbulent model was adopted with advection ADV 5 and transient analysis, corei-5, 4 Gb RAM computational resources.

In order to ensure close representation of the real life scenario, a non-impulsive start-up was adopted. The rotating region was initially set to have a known ideal speed. The simulation run was ramped up till this ideal speed was steady using calculated time step size relatively to the blade numbers. Having run the simulation to reach an ideal speed in rpm, the rotating region was set to free-spinning, while the mass moment of inertial of the turbine about the axis of rotation I_{zz} was also added as the inherent resistive force to rotation and further time steps were run until the steady state was reached, this was considered as the rotating speed of the impeller. The torque and rotating speed at the step were used to compute for power P_m using Eq. (9). The mechanical power P_m was assumed to be equal to electrical power to simplify the model (ideal generator, and speed deviation damper). The speed governing analysis, gear box configuration, and generator selection are not within the scope of this work.

The variations in the inlet and outlet flow velocity were also checked to determine flow reduction due to turbine insertion. The simulation was run for each peak and lean volumetric discharge rates. Therefore, two separate scenarios were considered for each input parameters, based on hydrofoil material. Stainless steel 304 was considered due to its global recommendation by World Health Organization as safe metal when comes in contact with edible substance. Aluminium 6061 was also considered due to its light weight coupled with its compounds significance in municipal water treatment [13].

3. Theory

The empirical formulae analyzed below describe the relevant mathematical expressions to this research. Parameters like blade solidity, tip speed ratio, hydrofoil profile equation of the turbine blade, the governing equation for the water distribution configuration and so on are analyzed.

3.1. Blade solidity

The blade solidity is an important design parameter for the axial flow impeller and is defined as the ratio of blade chord length to pitch.

$$\text{Blade Solidity} = c/s \tag{1}$$

where, $s = 2\pi r_m/Z_b$, r_m is the mean radius, Z_b is blade number, Cord length c is the length of the chord line and s is pitch. In case of an axial flow impeller mean radius is defined in terms of hub (r_h, inner radius) and tip radius (r_t, outer radius) as:

$$\left[(r_t^2 - r_h^2)/2\right]^{0.5} \tag{2}$$

Blade solidity affects various turbo machinery parameters. So to vary those parameters, the blade solidity has to be varied but there are some limitations imposed by Aspect ratio (wing) (span/chord), pitch. If an impeller has few blades i.e. high pitch it will result in less lift force and in a similar manner for more blades i.e. very low pitch, there will be high drag force, while rotor solidity is the ratio of the total area of the rotor blades to the swept area of the rotor [14].

3.2. Tip speed ratio

The tip-speed ratio (TSR) for turbine is the ratio between the tangential speed of the tip of a blade and the actual velocity of the fluid, v. This parameter is paramount in turbine power efficiency determination and given as [15]:

$$\lambda = (\omega * r)/v \tag{3}$$

where v is the water velocity, ω is angular speed and r is the radius of the turbine. In order words, the maximum power point of the turbine is close to lower tip speed ratio (TSR).

3.3. The hydrofoil cross-sectional profile

A symmetrical 4-digit series NACA airfoil, NACA 00xx foil, with "xx" being replaced by the percentage of thickness to chord length; the two first "00" digit indicates that there is no camber at both sides of the foil. According to Moran [16], Equation of NACA 0020 is given as;

$$y_t = 5tc\left[0.2969\sqrt{\frac{x}{c}} + (-0.1620)(x/c) + (-0.3516)(x/c)^2 + 0.2843(x/c)^3 + (-0.1015)(x/c)^4\right] \tag{4}$$

where c is the chord length, x is the position along the chord from 0 to c, y_t is the half thickness at a given value of x (centerline to surface), and t is the maximum thickness as a fraction of the chord (so 100 t gives the last two digits in the NACA 4-digit denomination.

3.4. Governing equations for fluid flow in the runner

The flow in the runner is assumed to be turbulent, and incompressible, the Reynolds Averaged Navier-Stokes (RANS) equations consisting of continuity, and momentum equations are significant to this analysis. In order to solve these governing equations numerically, there are simulation software like Analysis system workbench (ANSYS FLUENT), Autodesk Simulation CFD, Comsol Multiphysics and their solvers.

$$\text{continuity equ.} = \partial u_i/\partial x_i = 0 \tag{5}$$

$$\begin{aligned}\text{momentum equ.} &= \rho\partial u_i/\partial t + \rho\partial u_i u_j/\partial x_i \\ &= -\partial p/\partial xi + \partial/\partial x_i[\mu(\partial ui/\partial x_j + \partial uj/\partial x_i]\end{aligned} \tag{6}$$

$$\text{Energy equation} := \rho\partial t/\partial t + \rho\partial Tu_j/\partial x_j = \partial/c_p^{\partial x_j}(K^{\partial T})/\partial x_j \tag{7}$$

The governing equations for turbo machineries analysis are mostly non-linear which in turn have limited number of analytical solutions. Therefore, the approximate solutions are obtained by numerical methods [17].

3.5. Time steps calculation using blade passage

The blade-to-blade time step size t (s) is given by:

$$T = D/(N * 6) \tag{8}$$

3.6. Simulated mechanical power

The simulated mechanical power is obtained from the product of turbine torque and angular velocity of the turbine.

Table 1
Water distribution flow rate summary of the investigated sites.

Sites of Reference	Pipe diameter (m)	Peak Flow Rate (m^3/h)	Lean Flow Rate (m^3/h)
OAU	0.25	281	163
UI			
Amina Way	0.25	323	140
Stadium Reservoir	0.25	230	112
*FUTA			
(Jibowu)	0.1	288	72
(Hill top)			

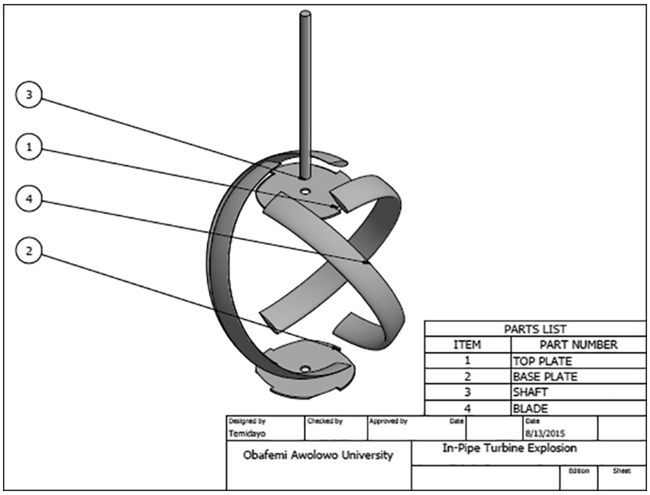

Fig. 2. Turbine exploded view.

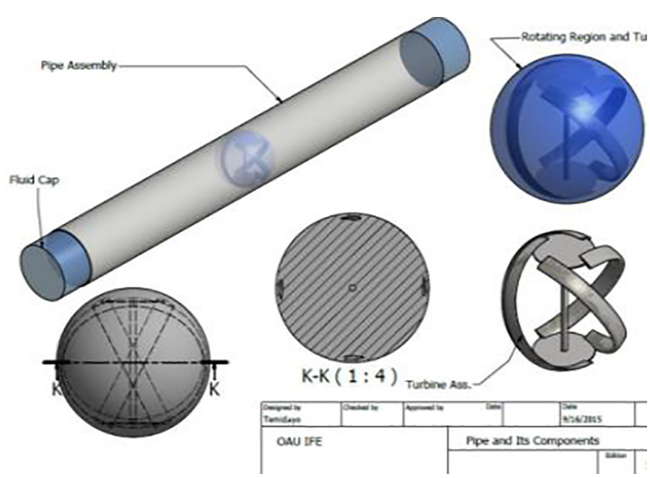

Fig. 3. In-pipe turbine assembly of rotating region.

Table 2
Mass Moment of Inertia Using CAD Software Autodesk Inventor [12].

Conduit Size (mm)	Mass Moment of Inertial of turbine model (kg-mm^2)	
	Aluminum (6061)	Stainless steel (3 0 4)
100	32.948	97.623
250	3635.587	10,647.269

$$P_m = T_s * \omega_s \tag{9}$$

where T_s, torque of the turbine shaft and ω_s is the angular speed of the shaft.

4. Results and discussion

The peak and the lean volumetric discharge of the water distribution networks of the tertiary institution considered were deduced from one hour interval time series of water distribution and tabulated below as Table 1.

The adaptive CAD model of in-pipe turbine is represented by Fig. 2 and Fig. 3 while Table 2 summarized the mass moment of inertia of the two turbines materials considered about the axis of rotation of the turbine. The computed power potential for peak and the lean distribution from the time series of distribution are presented by Tables 3–6 where it is deduced that the magnitude of the volumetric flow rate determines the turbine rotational speed or angular velocity as the case maybe.

The effective head $H_{effective}$ of the booster reservoirs considered, neglecting local losses due to unavailability of fittings details of the buried section of the pipe networks was estimated and summarized in Table 7 where the maximum and minimum effective head across investigated sites are 17.9 and 8 m respectively.

The particle trace display of the computational result is represented by Fig. 6 which enables a clear visualization of the fluid molecules agitation at the rotating region domain. The available heads with the corresponding head loss are also presented in the Table 7. The result of this study revealed that the fluid flow rate, effective head, the pipe diameter, hydrofoil profile, and turbine material determines the amount of hydropower harnessing potential in any water distribution system. The volumetric flow and pressure variation chart are represented by Figs. 4 and 5 respec-

Table 3
Peak Simulated Power for Stainless Steel Foil.

Study Area	Peak Discharge (m^3/h)	Pipe Diameter (m)	Torque N-m	Rotational Speed (rpm)	Rotational Speed (rad/s)	Power (Watt.)
OAU	281	0.25	28.8412	326.15	34.1543	985.05
UI						
Amina Way	323	0.25	30.8358	334.318	35.0097	1079.55
Stadium	230	0.25	28.7514	313.732	32.8539	944.60
*FUTA						
(Jibowu)	288	0.1	0.211771	365.174	38.2409	8.10
(Hill top)						

Table 4
Lean Simulated Power for Stainless Steel Foil.

Study Area	Lean Discharge (m^3/h)	Pipe Diameter (m)	Torque N-m	Rotational Speed (rpm)	Rotational Speed (rad/s)	Power (Watt)
OAU	163	0.25	17.77291	235.183	24.6283	437.72
UI						
Amina Way	140	0.25	15.1143	188.998	19.7918	299.14
Stadium Reservoir	112	0.25	15.0582	153.626	16.0877	242.25
*FUTA						
(Jibowu)	72	0.1	0.190648	98.0375	10.2665	1.96
(Hill top)						

Table 5
Peak Simulated Power for Aluminum Foil.

Study Area	Peak Discharge (m^3/h)	Pipe Diameter (m)	Torque N-m	Rotational Speed (rpm)	Rotational Speed (rad/s)	Power (Watt)
OAU	281	0.25	15.171	815.095	85.3565	1294.94
UI						
Amina Way	323	0.25	19.3068	822.663	86.1491	1663.26
Stadium Reservoir	230	0.25	13.6009	792.129	82.9516	1128.22
*FUTA						
(Jibowu)	288	0.1	0.224194	422.495	44.2436	9.92
(Hill top)						

Table 6
Lean Simulated Power for Aluminium Foil.

Study Area	Lean Discharge(m^3/h)	Pipe Diameter(m)	Torque N-m	Rotational Speed(rpm)	Rotational Speed(rad/s)	Power (Watt)
OAU	163	0.25	11.7055	732.509	76.7082	897.91
UI						
Amina Way	140	0.25	9.99686	639.489	66.9671	669.46
Stadium Reservoir	112	0.25	9.0434	438.958	45.9676	415.70
*FUTA						
(Jibowu)	72	0.1	0.171094	272.773	28.5647	4.89
(Hill top)						

Table 7
Head Loss Estimation for Stainless Steel and Aluminum Foil.

Booster Stations	Flow Rate(m^3/h)	Head Loss A (m)	Head Loss B (m)	Effective Head Available (m)	% Head Loss A	% Head Loss B
UI-1	112	0.7984	0.2664	13.70	5.79	1.94
UI-2	140	0.834 0	0.7287	17.90	4.66	4.05
OAU	163	0.8522	0.8278	16.00	5.33	5.17
UI-1	230	1.2993	1.1435	13.70	9.48	8.35
OAU	281	1.5518	1.4980	16.00	9.70	9.25
UI-2	323	1.7371	1.6273	17.90	9.70	9.09
FUTA-1	72	0.2985	0.3987	8.00	3.73	4.98
FUTA-1	288	7.6168	6.5526	8.00	95.21	81.91
FUTA-2	72*	0.2985	0.3987	12.30	2.43	3.24
FUTA-2	288*	7.6717	6.5526	12.30	61.93	53.27

Head Loss A: up to downstream pressure variation in the value of head for stainless steel foil (Pinlet-Pout)/ρg).
Head Loss B: up to downstream pressure variation in the value of head for aluminium foil (Pinlet-Pout)/ρg).

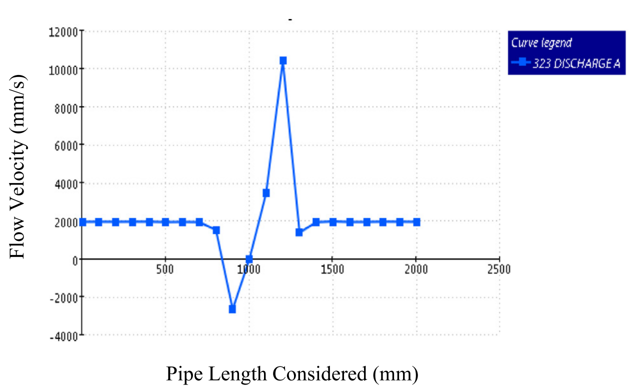

Fig. 4. 323 m^3/h volumetric flow rate velocity variations.

tively where turbine A represents a modeled turbine with hydrofoil of Stainless steel (3 0 4) material and turbine B foil is assigned material properties of aluminum 6061 respectively. Fig. 7 represents the vortices magnitude.

Considering summary Table 7, it is noticeable that the percentage head loss in 250 mm diameter fed pipe is less than 10 percent of the effective head available (Source and destination nodal points' topographic difference to ensure water get to destinations).

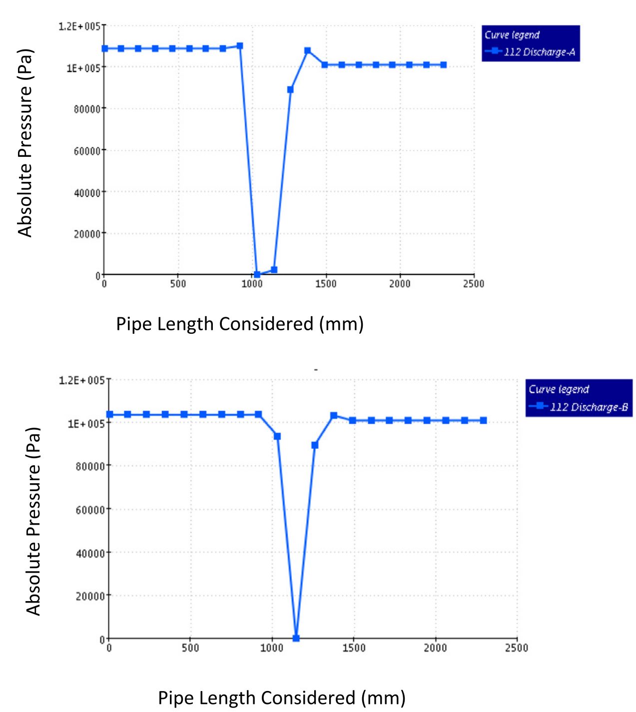

Fig. 5. Absolute pressure curve for 112 m^3/h volumetric discharge rate.

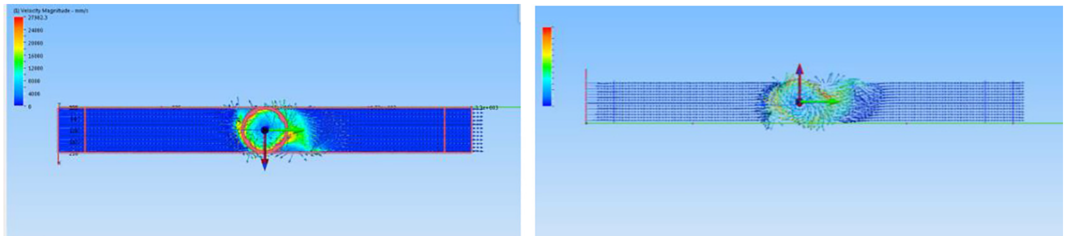

Fig. 6. Simulation Preview of Fluid Particles Trace (Autodesk Simulation CFD, 2015).

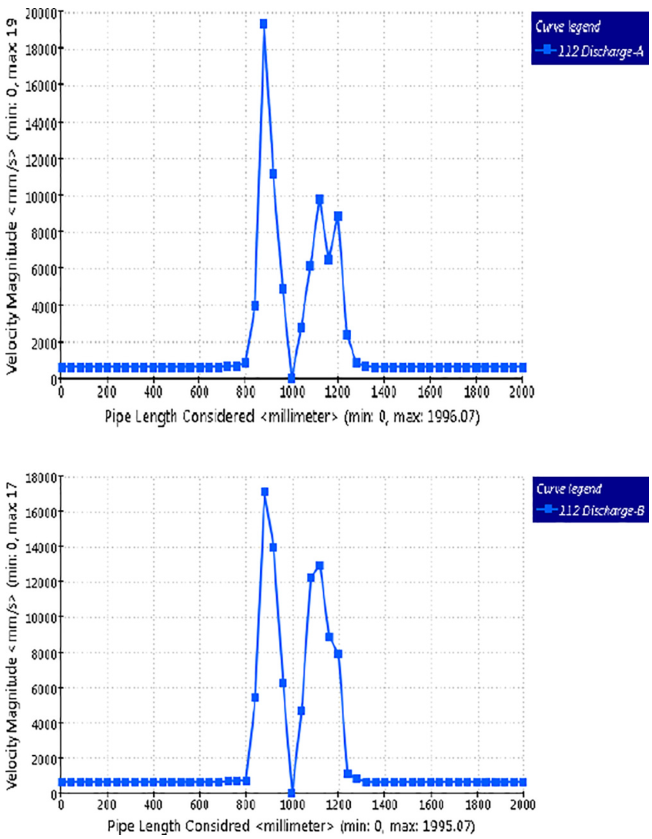

Fig. 7. Vorticity magnitude curve for 112 m^3/h volumetric discharge rate.

However, for 100 mm diameter fed distribution mains the percentage of effective head loss is as high as 95 percent for stainless steel turbine blades which signifies in-pipe turbine power harnessing as the function of the turbine materials and the pipe diameter in question. The Configuration efficiency curve can be deduced from Table 7 due to inextricability of the percentage head loss to the turbine efficiency. The efficiency of the turbine is inversely proportional to percentage head loss while percent head loss increases as pipe diameter decreases. The volumetric flow rate variations curve indicates velocity drop at the turbine insertion point within the analysis domain with appreciable velocity recovery at downstream. The same effect is on the absolute pressure in the system. The vorticity magnitude at the turbine insertion region is high and this calls for a careful configuration of flow deflection at the turbine insertion point to prevent cyclic stress on the equipment.

5. Conclusions

The simulated power of stainless steel foil for the reservoir-fed distribution networks yielded 242 and 1080 W, for the lean and peak periods, respectively; the corresponding values with aluminium foil are 415 and 1663 W in 250 mm diameter fed distribution pipe. However, lower magnitude of derived power was obtained in 100 mm diameter fed pipe coupled with high head loss. A stringent comparison of the results obtained in this study revealed that hydropower harnessing capacity in water distribution line is the function of parameters like pipe diameter, turbine blades materials and the flow rate in the pipe.

Future analysis may involve the effects and the benefits of multiple in-pipe turbine installations along the line. The turbulent intensity and vortices magnitude curve in each of the scenario in the computational analysis in this work implies that there are high vortices at the impeller region that might cause cyclic stress (surface fatigue) on the impellers to get above unsaved threshold, further work can look into in-pipe turbine design optimization, water network configuration by further improvement in upstream and downstream deflections design at the turbine insertion point. Generator selection for in line power generation may also be considered. Finally, economic viability and the cost of implementation of hydropower harnessing in water line can also be research upon.

Acknowledgements

My profound gratitude goes to Almighty God for the privilege given to conclude this research. I also appreciate the administration of the institutions visited for data gathering by using their water distribution equipment. I finally appreciate Prototype Engineering Development Institute, Nigeria for the opportunity (release to further) accorded to pursue my M. Sc. because this paper was derived from one of the M. Sc. research objectives.

References

[1] ESHA, European Small Hydropower Association, Energy Recovery in Existing Infrastructureswith Small Hydropower Plants: Multipurpose Schemes Overview and Examples, 2010, http:// www.intechopen.com/download/pdf/3140. Accessed jun., 2014.
[2] V. Sammartano, C. Aric'o, A. Carravetta, O. Fecarotta, T. Tucciarelli, Banki-michell optimal design by computational fluid dynamics testing and hydrodynamic analysis, Energies 6 (5) (2013) 2362–2385.
[3] H. Ramos, M. Mello, P. De, Clean power in water supply systems as a sustainable solution: from planning to practical implementation, Water Sci. Technol. 10 (1) (2010) 39–49.
[4] A. Carravetta, G. Del Giudice, O. Fecarotta, H. Ramos, Pat design strategy for energy recovery in water distribution networks by electrical regulation, Energies 6 (1) (2013) 411–424.
[5] J. Chen, H.X. Yang, C.P. Liu, C.H. Lau, M. Lo, A novel vertical axis water turbine for power generation from water pipelines, Energy (54) (2013) 184–193.
[6] Aline Choulot Vincent Denis, Petras Punys, Integration of Small Hydro Turbines into Existing Water Infrastructures, Hydropower Practice and Application, Dr. Hossein Samadi Boroujeni (Ed.), 2012, ISBN: 97895351 0164 2, InTech, pp. 243–244. Available from: http://www.intechopen.com/books/hydropower-practice-andapplication/.
[7] R.A. Schlabach, M.R. Cosby, E. Kurth, I. Palley, G. Smith, In-Pipe Hydro-Electric Power System and Turbine, US Patent Application Publication, (Northwest Pipe and Lucid Energy), 2011. Patent (10) Patent No.: US 7,959,411 B2.
[8] I. Samora, V. Hasmatuchi, C. Münch-Alligné, M.J. Franca, A.J. Schleiss, H.M. Ramos, Experimental characterization of a five blade tubular propeller turbine for pipe inline installation, Renew. Energy 95 (2016) 356–366, https://doi.org/10.1016/j.renene.2016.04.023.

[9] O.A. Koya, T.L. Oladosu, Hydropower potentials of water distribution networks in some public universities: a case study, Leonardo Electr. J. Practices Technol. Issue 30, ISSN 1583–1078 (2017) 287–298.
[10] Autodesk Inventor, Autodesk Inventor Professional, Produced by Autodesk Inc., 2015, Web page available at: www.autodesk.com/inventor.
[11] Elster Kent H4000, Elster Water Metering Limited 130 Camford Way, Sundon Park Luton, shire, L3 3AN United Kingdom. http://www.elstermetering.com
[12] Autodesk Simulation CFD, Autodesk Simulation CFD, Produced by Autodesk Inc., 2015, Web page available at: www.autodesk.com/cfd
[13] U.S. Environmental Protection Agency, Energy Conservation Measures and Technologies for Municipal Waste Water Treatment Facilities, 2010, http://water.epa.gov/scitech/wastetech/upload/Evaluation-of-Energy-Conservation-Measures-for-Wastewater-Treatment-Facilities.pd.
[14] Peng, W. William, Fundamentals of Turbomachinery, Wiley, 2008, ISBN 978-0-470-12422-2
[15] I. Paraschivoiu, Wind Turbine Design with Emphasis on Darrieus Concept, 1st ed., Polytechnic International, Montreal, Quebec, Canada, 2002.
[16] J. Moran, An Introduction to Theoretical and Computational Aerodynamics, Dover Publications, 2003, ISBN 0-486-42879-6, p. 7.
[17] R.I. Lewis, Turbo Machinery Performance Analysis (Arnold London), Lucid (2014), 1996, Lucid Energy, Inc, http://www.lucidenergy.com. Accessed 4h of February, 2014.